Functional Imaging of Neuroendocrine Tumors: A Head-to-Head Comparison of Somatostatin Receptor Scintigraphy, ^{123}I-MIBG Scintigraphy, and ^{18}F-FDG PET

Tina Binderup[1,2], Ulrich Knigge[2,3], Annika Loft[1], Jann Mortensen[1], Andreas Pfeifer[1,2], Birgitte Federspiel[4], Carsten Palnaes Hansen[3], Liselotte Højgaard[1,2], and Andreas Kjaer[1,2]

[1]Department of Clinical Physiology, Nuclear Medicine and PET, Rigshospitalet, Copenhagen, Denmark; [2]Cluster for Molecular Imaging, Faculty of Health Sciences, University of Copenhagen, Copenhagen, Denmark; [3]Department of Surgical Gastroenterology, Rigshospitalet, Copenhagen, Denmark; and [4]Department of Pathology, Rigshospitalet, Copenhagen, Denmark

Functional techniques are playing a pivotal role in the imaging of cancer today. Our aim was to compare, on a head-to-head basis, 3 functional imaging techniques in patients with histologically verified neuroendocrine tumors: somatostatin receptor scintigraphy (SRS) with ^{111}In-diethylenetriaminepentaacetic acid-octreotide, scintigraphy with ^{123}I-metaiodobenzylguanidine (MIBG), and ^{18}F-FDG PET. **Methods:** Ninety-six prospectively enrolled patients with neuroendocrine tumors underwent SRS, ^{123}I-MIBG scintigraphy, and ^{18}F-FDG PET on average within 40 d. The functional images were fused with low-dose CT scans for anatomic localization, and the imaging results were compared with the proliferation index as determined by Ki67. **Results:** The overall sensitivity of SRS, ^{123}I-MIBG scintigraphy, and ^{18}F-FDG PET was 89%, 52%, and 58%, respectively. Of the 11 SRS-negative patients, 7 were ^{18}F-FDG PET-positive, of which 3 were also ^{123}I-MIBG scintigraphy–positive, giving a combined overall sensitivity of 96%. SRS also exceeded ^{123}I-MIBG scintigraphy and ^{18}F-FDG PET based on the number of lesions detected (393, 185, and 225, respectively) and tumor subtypes. ^{123}I-MIBG scintigraphy was superior to ^{18}F-FDG PET for ileal neuroendocrine tumors, and ^{18}F-FDG PET was superior to ^{123}I-MIBG scintigraphy for pancreaticoduodenal neuroendocrine tumors. The sensitivity of ^{18}F-FDG PET (92%) exceeded that of both SRS (69%) and ^{123}I-MIBG scintigraphy (46%) for tumors with a proliferation index above 15%. **Conclusion:** The overall sensitivity of ^{123}I-MIBG scintigraphy and ^{18}F-FDG PET was low compared with SRS. However, for tumors with a high proliferation rate, ^{18}F-FDG PET had the highest sensitivity. The results indicate that, although SRS should still be the routine method, ^{18}F-FDG PET provides complementary diagnostic information and is of value for neuroendocrine tumor patients with negative SRS findings or a high proliferation index.

Received Aug. 25, 2009; revision accepted Feb. 4, 2010.
For correspondence or reprints contact: Andreas Kjaer, Rigshospitalet, Department of Clinical Physiology, Nuclear Medicine and PET, 4011, Blegdamsvej 9, 2100 Copenhagen Ø, Denmark.
E-mail: kjaer@mfi.ku.dk

Key Words: neuroendocrine tumors; somatostatin receptor scintigraphy; ^{123}I-MIBG scintigraphy; ^{18}F-FDG PET

J Nucl Med 2010; 51:704–712
DOI: 10.2967/jnumed.109.069765

The presence of prominent molecular biomarkers makes neuroendocrine tumors attractive for functional imaging with PET and SPECT and for treatment with peptide receptor radionuclide therapy. In particular, somatostatin receptors have been found to be overexpressed in these tumors, with subtype 2 being predominant (*1,2*). Other biomarkers are also overexpressed in these tumors, such as dopamine receptors (*3*) and molecules in relation to the monoamine pathways (*4*), and these can also be used as imaging targets.

The current gold standard for functional imaging of neuroendocrine tumors is somatostatin receptor scintigraphy (SRS) with ^{111}In-diethylenetriaminepentaacetic acid-octreotide (*4,5*), targeting the somatostatin receptors with the highest affinity for subtype 2. The increased monoamine metabolism also observed in neuroendocrine tumors can be visualized by the ^{123}I-labeled noradrenalin analog metaiodobenzylguanidine (MIBG). Cellular uptake of ^{123}I-MIBG is mediated by the noradrenalin transporter, and intracellular uptake in secretory vesicles is mediated by the vesicular monoamine transporter. Imaging of neuroendocrine tumors with ^{123}I-MIBG is used as an alternative to SRS (*6,7*), but apart from pheochromocytomas, in which ^{123}I-MIBG has shown excellent sensitivity, the selection criteria for other neuroendocrine tumors are unsettled.

For functional imaging of cancer in general, ^{18}F-FDG PET is without comparison the most widely used nuclear medicine technique. However, ^{18}F-FDG PET has never been used on a routine basis for imaging of neuroendocrine

tumors, and its diagnostic performance is unsettled. A few smaller studies on neuroendocrine tumor patients have indicated that ^{18}F-FDG PET might be of value for tumors with a high proliferation index, whereas the diagnostic sensitivity seems to be low for neuroendocrine tumors with a low proliferation index, slow growth rate, and low glucose consumption (*8–10*). However, the small sample size of the studies requires further investigation of the real sensitivity of ^{18}F-FDG PET for neuroendocrine tumor imaging in comparison with traditionally used functional imaging scans.

Many promising new tracers have been developed for imaging of cancer in general (*11,12*), as well as for neuroendocrine tumors in particular (*13–15*). However, SRS, ^{123}I-MIBG scintigraphy, and ^{18}F-FDG PET remain the 3 molecular imaging techniques most widely available and with the most comprehensive clinical experience for neuroendocrine tumors and cancer in general. A direct head-to-head comparison of these 3 scintigraphy techniques has, to the best of our knowledge, not been undertaken in a large prospective study. The aim of this study was to perform such a comparison in a large group of prospectively enrolled patients with histologically verified neuroendocrine tumors.

MATERIALS AND METHODS

Between May 2007 and June 2008, 96 consecutive patients with neuroendocrine tumors (45 men and 51 women; mean age, 60 y; range, 34–81 y) were prospectively enrolled in the study at the Department of Surgical Gastroenterology C, Copenhagen University Hospital, Rigshospitalet. Rigshospitalet is one of 2 secondary-to-tertiary referral centers for treatment of patients with neuroendocrine tumors in Denmark. Patients are referred to this center for treatment and follow-up after the initial diagnosis. The histopathologic diagnoses were neuroendocrine tumor of the ileum (45 cases), pancreas or duodenum (functioning or nonfunctioning; 29 cases), lung (typical or atypical; 7 cases), colon (6 cases), gallbladder (1 case), and stomach (1 case). In addition, 7 patients had liver metastases whose primary neuroendocrine tumor was of unknown origin. Patient characteristics are shown in Table 1.

TABLE 1. Patient Characteristics

Characteristic	Data
Sex (*n*)	
Male	45 (47%)
Female	51 (53%)
Mean age (y)	
At diagnosis	56 (range, 33–81)
At scanning time	60 (range, 34–81)
Median time (±SD) from diagnosis (mo)	26 ± 63
Primary tumor removed (*n*)	
Yes	36 (38%)
No	55 (57%)
Nonradical operation	5 (5%)
Type of tumor (*n*)	
Ileal neuroendocrine tumor	45 (47%)
Colonic neuroendocrine tumor	6 (6%)
Pancreaticoduodenal neuroendocrine tumor	29 (30%)
Typical and atypical bronchial neuroendocrine tumor	7 (7.5%)
Other and unknown primary with metastases	9 (9.5%)
Image-verified metastatic disease at scanning time (*n*)	
Yes	84 (88%)
No	12 (12%)
CT-verified liver metastases (*n*)	
Yes	61 (64%)
No	35 (36%)
Mean lesion size on CT (cm, $n = 81$)	3.99 (range, 0.7–18.9)
Ki67 proliferation index (*n*)	
≤2%	46 (48%)
>2% ≤ 15%	26 (27%)
>15%	13 (14%)
Missing	11 (11%)
Treatment (*n*)	
Somatostatin analog	27 (28%)
α-Interferon	29 (30%)
Chemotherapy, 5-fluorouracil/streptozotocin	25 (26%)
Chemotherapy, other	7 (7%)
Radiofrequency ablation	5 (5%)
Liver embolization	4 (4%)
Peptide receptor radionuclide therapy	28 (29%)

Inclusion criteria were the presence of histologically verified neuroendocrine tumors of gastroenteropancreatic or bronchopulmonary origin (typical and atypical bronchial neuroendocrine tumors) and the presence of primary, residual, or recurrent disease (primary tumor, metastases, or both) on enrollment in the study.

Written informed consent was obtained from all participants, and the study was approved by the regional scientific ethical committee.

All aspects of patient care and treatment were performed at the discretion of the treating clinicians and according to routine procedures of the department, which are in accordance with the guidelines of the European Neuroendocrine Tumour Society (*16*).

SRS

SRS was performed according to a previously described procedure (*17*). In brief, a dose of 166–269 MBq of ^{111}In-diethylenetriaminepentaacetic acid-octreotide (OctreoScan; Mallinckrodt) was injected intravenously. After 24 h, anterior and posterior whole-body scans were acquired with the patient supine. Scans were performed at a speed of 5 cm/min and a matrix size of 256 × 1,024 using a dual-head γ-camera equipped with a medium-energy general-purpose parallel-hole collimator and a low-dose CT unit (VG Hawkeye; GE Healthcare, or Precedence 16-slice scanner; Philips Healthcare). The CT acquisition requires minutes with the VG Hawkeye but only seconds with the Precedence. Accordingly, the CT images obtained with the VG Hawkeye are more blurred because of breathing of the patients during image acquisition. Static images were acquired after 48 h. Images were acquired over 15 min, with a matrix size of 256 × 256. SPECT was performed after 24 h using 6° steps, 40 s/step, a 180° orbit, and a matrix size of 128 × 128. The SPECT images were fused with the simultaneously obtained low-dose CT images using the

eNTEGRA (GE Healthcare) or Jetstream (Philips) workstation. The low-dose CT images were used as anatomic guides for localization of the pathologic foci and for attenuation correction.

^{123}I-MIBG Scintigraphy

One hour before injection of the radioisotope, 130 mg of potassium iodide were administered perorally to minimize ^{123}I uptake in the thyroid gland. A dose of 150–266 MBq of ^{123}I-MIBG was injected intravenously. After 24 h, anterior and posterior whole-body scans were acquired using a dual-head camera with a low-energy general-purpose parallel-hole collimator, favoring higher sensitivity (*18,19*), and a low-dose CT unit (VG Hawkeye or Precedence 16-slice) with the patient supine. Static images were acquired over 15 min with a matrix size of 256 × 256. SPECT was performed after 24 h using 6° steps, 40 s/step, a 180° orbit, and a matrix size of 128 × 128. The SPECT images were fused with the low-dose CT images.

^{18}F-FDG PET

PET/CT images were acquired 1 h after injection of 342–467 MBq of ^{18}F-FDG. Blood glucose was measured before the ^{18}F-FDG injection, and for all patients, the level was no more than 8 mmol/L.

PET/CT was performed using a Discovery LS scanner (GE Healthcare) or a Biograph 16 scanner (Siemens). The emission scanning time was 3 min per bed position. The CT scans were low-dose with 10 mAs for minimization of the radiation burden. The CT acquisition time of the PET/CT scanners was comparable to that of the Precedence SPECT/CT scanner (a few seconds). The CT data were used for attenuation correction of the PET data and as anatomic guides for localization of the pathologic foci. The PET and low-dose CT images were reconstructed in all 3 planes and fused and analyzed on an eNTEGRA PET workstation and Leonardo workstation (Siemens), respectively. All patients were instructed to fast for at least 6 h before the ^{18}F-FDG injection.

Immunohistochemical Evaluation of Ki67

Formalin-fixed paraffin-embedded tissue sections 4 μm thick were cut and mounted on coated slides. Antigens were retrieved with target retrieval solution, high pH, for 20 min at 97°C (code K8002; Dako) using the Dako pretreatment link. After blocking of endogenous peroxidase activity with EnVision FLEX+ (code K8002; Dako) for 5 min, tissue sections were incubated with monoclonal mouse antihuman Ki67 antigen (code M7240; Dako) at a dilution of 1:200 for 20 min at room temperature.

The reaction was visualized using EnVision FLEX+ mouse link for 15 min followed by EnVision FLEX+ horseradish peroxidase for 20 min and finally EnVision FLEX+ diaminobenzidine for 10 min. The sections were counterstained with hematoxylin for 1 min. A section of the human tonsil was used as a positive control. The number of positive tumor nuclei per 100 tumor cells was counted. Based on the location of the primary tumor, histopathologic findings, and proliferation index, tumors were graded according to the World Health Organization 2000 classification (*20*).

Data Analysis and Statistics

The 3 scintigraphy techniques were, on average, performed within 40 d in a random order for each patient and interpreted according to our clinical routine procedure by 2 nuclear medicine physicians. Image interpretation was analyzed on a patient basis as positive or negative, on a region basis by counting the number of lesions in a specific region, and on a lesion basis by counting the total number of lesions detected by each scintigraphy technique. If more than 5 lesions were visualized by 1 of the 3 scans, the number of lesions was truncated at 5 for that region according to the response evaluation criteria in solid tumors (*13,14,21,22*). Because only patients known to have primary, metastatic, or residual disease on image acquisition were included in the study, the overall sensitivity of each scintigraphy technique was calculated as the number of patients with at least 1 positive finding divided by the number of patients included.

As part of the routine follow-up, patients were followed by diagnostic CT of the abdomen or thorax every 6–12 mo. Relevant CT images were available for 94 patients. Immunohistochemical staining for the proliferation marker Ki67, which is considered important for initial staging and diagnosis of neuroendocrine tumors (*16*), was available for 85 patients.

For statistical analyses of the sensitivities of the 3 scintigraphy technique, 2 × 2 tables were created and a χ^2 test was used to analyze statistically significant differences. A paired t test was used for testing the difference between the average numbers of lesions detected by each scintigraphy technique for a certain region.

All data analyses were performed using SPSS software, version 16.0 (SPSS Inc.). P values of less than 0.05 were considered significant.

RESULTS

Patient-Based Analysis

The results for the 96 patients imaged with SRS, ^{123}I-MIBG scintigraphy, and ^{18}F-FDG PET were evaluated. The overall sensitivities of SRS, ^{123}I-MIBG scintigraphy, and ^{18}F-FDG PET for detection of either primary tumor or metastases were 89%, 52%, and 58%, respectively. In 14 patients (15%), SRS was the only scintigraphy technique revealing pathologic foci. Of the 96 included patients, 11 were SRS-negative, and of these, 7 were ^{18}F-FDG PET–positive and 3 were ^{123}I-MIBG scintigraphy–positive. The 3 patients with positive ^{123}I-MIBG scintigraphy results were also ^{18}F-FDG PET–positive. Thus, in no case was ^{123}I-MIBG scintigraphy the only technique with positive results. With the results of all 3 scintigraphy techniques combined, the overall sensitivity was 96% (92/96). The remaining 4 patients, in whom all 3 scintigraphy techniques had negative results, were confirmed to have a neuroendocrine tumor either by contrast-enhanced diagnostic CT or by endoscopy with confirmation afterward by surgical removal of the tumor. The results of ^{123}I-MIBG scintigraphy and ^{18}F-FDG PET for patients in whom SRS was positive and negative is shown in Tables 2 and 3, respectively.

Lesion-Based Analysis

A total of 393 lesions were detected by SRS, in comparison with 185 lesions detected by ^{123}I-MIBG scintigraphy and 225 lesions detected by ^{18}F-FDG PET. All 3 scintigraphy techniques detected most lesions in the liver, followed by lesions in lymph nodes (Fig. 1). SRS and ^{18}F-FDG PET both had a significantly higher detection rate

TABLE 2. Distribution of ^{123}I-MIBG Scintigraphy and ^{18}F-FDG PET Results for Patients with Positive SRS Findings (n = 85)

	^{18}F-FDG result		
^{123}I-MIBG result	Negative	Positive	Total
Negative	14	24	38
Positive	22	25	47
Total	36	49	85

for lymph node lesions than did ^{123}I-MIBG scintigraphy ($P < 0.001$), whereas there was no significant difference between SRS and ^{18}F-FDG PET for lymph node detection ($P = 0.185$). For detection of liver metastases, SRS was significantly better than both ^{18}F-FDG PET and ^{123}I-MIBG scintigraphy ($P < 0.001$), whereas no significant difference was found between the ability of ^{18}F-FDG PET and ^{123}I-MIBG scintigraphy to reveal liver metastases. For detection of bone metastases, SRS was also significantly better than ^{18}F-FDG PET ($P = 0.011$) and ^{123}I-MIBG scintigraphy ($P < 0.001$), whereas ^{18}F-FDG PET seems more sensitive than ^{123}I-MIBG scintigraphy although the difference is only borderline significant ($P = 0.063$). SRS detected significantly more lesions in the pancreas than did ^{123}I-MIBG scintigraphy ($P = 0.042$), but there was no significant difference between SRS and ^{18}F-FDG PET or between ^{18}F-FDG PET and ^{123}I-MIBG scintigraphy in the ability to detect pancreatic lesions. The sensitivities of the 3 scintigraphy techniques were not significantly different for detection of intestinal and thoracic lesions. As shown in Table 4, all patients with CT-verified bone metastases had positive ^{18}F-FDG PET findings, and of the 29 patients with 5 or more liver lesions detected by CT, 22 (76%) were ^{18}F-FDG PET–positive.

Analysis Based on Tumor Origin

Based on tumor origin, the sensitivity of SRS, ^{123}I-MIBG scintigraphy, and ^{18}F-FDG PET was 91%, 71%, and 36%, respectively, for ileal neuroendocrine tumors; 90%, 31%, and 79%, respectively, for pancreaticoduodenal neuroendocrine tumors; 86%, 57%, and 71%, respectively, for bronchopulmonary-neuroendocrine tumors; 67%, 17%, and 83%, respectively, for colonic neuroendocrine tumors; and 100%, 43%, and 86%, respectively, for liver metastases with an unknown primary tumor. The neuroendocrine tumor of the gallbladder was SRS- and ^{123}I-MIBG scintigraphy–positive and ^{18}F-FDG PET–negative, whereas the neuroendocrine tumor in the stomach was positive only on ^{18}F-FDG PET (Table 5).

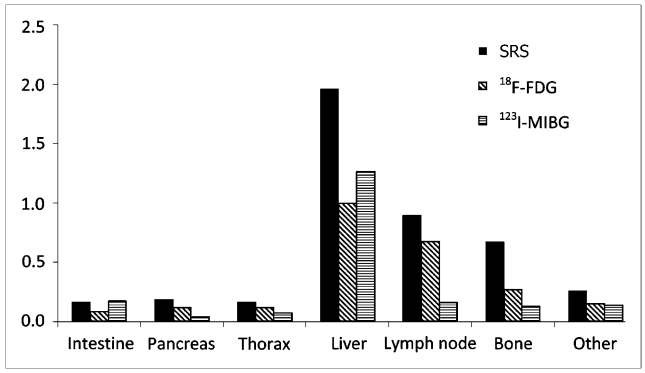

FIGURE 1. Comparison of average number of foci identified by SRS, ^{123}I-MIBG scintigraphy, and ^{18}F-FDG PET in different regions of body.

Analysis Based on Proliferation Index

The sensitivity of the 3 scintigraphy techniques was analyzed according to the proliferation index, which was available for 85 patients (89%) as shown in Table 6. The proliferation index was below 2% in 46 patients, 2%−15% in 26 patients, and above 15% in 13 patients. For SRS and ^{123}I-MIBG scintigraphy, there was no significant difference in sensitivity between tumors with a proliferation index below 2% and those above 2% (87% vs. 87% for SRS and 48% vs. 64% for ^{123}I-MIBG scintigraphy). The sensitivity of ^{18}F-FDG PET was significantly higher for tumors with a proliferation index above 2% (80% vs. 41%, χ^2 test, $P < 0.001$). When the proliferation index was dichotomized to above or below 15%, the sensitivity of ^{18}F-FDG PET increased to 92% for tumors with a proliferation index above 15%, compared with 53% for tumors with a pro-

TABLE 3. Distribution of ^{123}I-MIBG Scintigraphy and ^{18}F-FDG PET Results for Patients with Negative SRS Findings (n = 11)

Patient no.	^{18}F-FDG result	^{123}I-MIBG result	Lesion size on CT (cm)	Proliferation index
1	Positive	Positive	5.6	75
2	Positive	Positive	4.0	1.5
3	Positive	Positive	0.9	2.5
4	Positive	Negative	5.0	95
5	Positive	Negative	4.7	2.0
6	Positive	Negative	Carcinosis	50
7	Positive	Negative	Negative on CT	90
8	Negative	Negative	2.0	1.0
9	Negative	Negative	1.9	0.5
10	Negative	Negative	0.8	1.5
11	Negative	Negative	0.8	1.5

TABLE 4. Metastatic Burden Assessed by Diagnostic CT for ^{18}F-FDG PET–Negative Group (n = 38) and ^{18}F-FDG PET–Positive Group (n = 54)

	Liver			Lymph nodes			Bone		
Group	0 METs	1–4 METs	≥5 METs	0 METs	1–4 METs	≥5 METs	0 METs	1–4 METs	≥5 METs
^{18}F-FDG–positive	16 (52)	16 (50)	22 (76)	32 (59)	15 (52)	7 (78)	44 (54)	8 (100)	2 (100)
^{18}F-FDG–negative	15 (48)	16 (50)	7 (24)	22 (41)	14 (48)	2 (22)	38 (46)	0 (0)	0 (0)

METs = metastases.
Data are numbers of metastases, with percentages in parentheses.

liferation index below 15% (χ^2 test, $P = 0.008$). In contrast, the sensitivity of SRS was significantly higher for tumors with a proliferation index below 15% (90% vs. 69%, χ^2 test, $P = 0.037$). For ^{123}I-MIBG scintigraphy, there was no significant difference in sensitivity between neuroendocrine tumors with a Ki67 below 15% and those above 15% (57% vs. 46%, χ^2 test, $P = 0.471$). For patients with a proliferation index between 2% and 15% ($n = 26$), at least 1 of the 3 scintigraphy techniques revealed pathologic foci: only 1 patient was SRS-negative, but the patient was ^{18}F-FDG PET– and ^{123}I-MIBG scintigraphy–positive. Of the 26 patients with a proliferation index between 2% and 15%, 7 were ^{123}I-MIBG scintigraphy–negative but ^{18}F-FDG PET–positive, 7 were ^{123}I-MIBG scintigraphy–positive but ^{18}F-FDG PET–negative, and 11 were identified by all 3 scintigraphy techniques. Examples of the imaging results of the 3 modalities for 3 patients with different Ki67 indexes are shown in Figures 2–4.

DISCUSSION

Functional imaging based on radiolabeled analogs targeting overexpressed receptors and transporters is playing a pivotal role in imaging of cancer today. Because of a frequent overexpression of specific molecular markers in neuroendocrine tumors, they are one of the most widely imaged despite their relatively low incidence (2–5/100,000 inhabitants) (*23–25*).

The low incidence of neuroendocrine tumors represents a significant scientific challenge to the design of the study and the size of the investigated population. Therefore, most studies with functional imaging of neuroendocrine tumor patients are retrospective and have small populations. ^{123}I-MIBG scintigraphy and SRS have been compared only in retrospective studies (*6,26*), and most studies of ^{18}F-FDG PET in neuroendocrine tumor have included few patients (*8,9*). In a recent and larger study, ^{18}F-FDG PET seemed valuable for aggressive neuroendocrine tumors, but conclusions were based on only 6 patients, all having high-grade tumors (*10*). In the present study, we prospectively enrolled 96 patients diagnosed with neuroendocrine tumors and made a direct head-to-head comparison of the 3 types of functional imaging: SRS, ^{123}I-MIBG scintigraphy, and ^{18}F-FDG PET. Twenty-six patients had a Ki67 index between 2% and 15% (well-differentiated neuroendocrine carcinomas), and 13 patients had a Ki67 index above 15% (poorly differentiated neuroendocrine carcinomas) according to the World Health Organization classification (*16*).

The results of our study revealed that the sensitivity of SRS for detection of neuroendocrine primary tumors and metastases exceeds the sensitivity of ^{123}I-MIBG scintigraphy and ^{18}F-FDG PET both overall and with regard to the ability to detect lesions in different body regions and based on the origin of the neuroendocrine tumor. The number of regions detected by SRS, ^{123}I-MIBG scintigraphy, and ^{18}F-FDG PET varied substantially between the 3 scintigraphy techniques, with 393 lesions detected by SRS, 185 detected by ^{123}I-MIBG scintigraphy, and 225 detected by ^{18}F-FDG PET. Because SRS detected more than twice as many lesions as ^{123}I-MIBG scintigraphy, there is no doubt that the ligand of choice for diagnostic imaging and radionuclide therapy should be a somatostatin analog, as is also the current standard (*25,27*). The overall sensitivity of 89% for SRS and 52% for ^{123}I-MIBG scintigraphy in the present study fully agrees with our previous molecular biology study of neuroendocrine tumors (*1*). That study found most

TABLE 5. Sensitivity of Functional Imaging Results Based on Origin of Tumor

Origin of tumor	SRS	^{123}I-MIBG	^{18}F-FDG
Ileal neuroendocrine (n = 45)	91% (41)	71% (32)	36% (16)
Pancreaticoduodenal neuroendocrine (n = 29)	90% (26)	31% (9)	79% (23)
Neuroendocrine of lung (n = 7)	86% (6)	57% (4)	71% (5)
Colonic neuroendocrine (n = 6)	67% (4)	17% (1)	83% (5)
Unknown or rare origin (n = 9)	89% (8)	44% (4)	78% (7)
Total	89% (85)	52% (50)	58% (56)

Data in parentheses are numbers of patients.

TABLE 6. Functional Imaging Results Based on Proliferation Index

	SRS		^{123}I-MIBG		^{18}F-FDG	
Ki67 value	Positive	Negative	Positive	Negative	Positive	Negative
<2%	87% (40)	13% (6)	48% (22)	52% (24)	41% (19)	59% (27)
2%–15%	96% (25)	4% (1)	73% (19)	27% (7)	73% (19)	27% (7)
>15%	69% (9)	31% (4)	46% (6)	54% (7)	92% (12)	8% (1)

Data in parentheses are numbers of patients.

neuroendocrine tumors to have a high somatostatin receptor subtype 2 expression, but only 50% of the tumors had overexpression of the noradrenalin transporter, which mediates uptake of ^{123}I-MIBG into cells.

Determination of the proliferation index is one of the crucial diagnostic procedures for correct staging of neuroendocrine tumors (*28,29*). In the present study, the sensitivity of SRS and ^{18}F-FDG PET was significantly different for tumors with different proliferation indexes. For tumors with a proliferation index above 15%, ^{18}F-FDG PET had a sensitivity of 92%, which greatly exceeded the performance of both SRS and ^{123}I-MIBG scintigraphy, with sensitivities of 69% and 46%, respectively. Use of ^{18}F-FDG as an imaging tracer should be considered in these cases, because these aggressive tumors are missed in a substantial number of patients and the degree of dissemination of the disease may be underestimated. If the disease is considered less disseminated than it is, a suboptimal treatment will likely be chosen because only the most aggressive cases are treated with systemic chemotherapy; most patients (with less aggressive disease) are treated with somatostatin analogs or α-interferon (*16*).

Patients with a substantial metastatic burden were in most cases ^{18}F-FDG PET–positive. Thus, 76% of patients with 5 or more liver lesions and all patients with bone metastases were ^{18}F-FDG PET–positive. However, ^{18}F-FDG PET was also positive in approximately 50% of patients with no liver metastases and 60% of patients with no CT-verified lymph node metastases.

In 7 SRS-negative patients, ^{18}F-FDG PET was positive, and 3 of these were also ^{123}I-MIBG scintigraphy–positive. In 4 of these patients, the proliferation index was above 15% and loss of somatostatin receptor expression due to dedifferentiation of the tumor could explain the negative SRS findings.

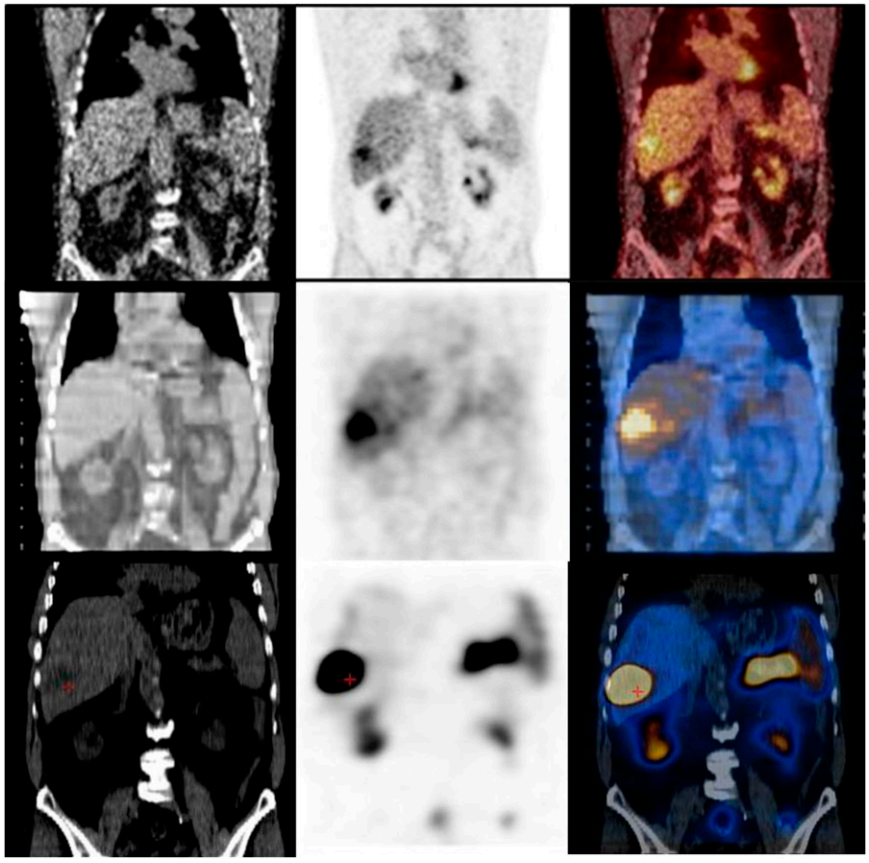

FIGURE 2. Patient in whom the 3 imaging modalities were in agreement with each other, finding large focus in liver. Origin of primary tumor and liver metastases was unknown. Ki67 index was 10%. From left to right are CT images; ^{18}F-FDG PET (top), ^{123}I-MIBG scintigraphy (middle), and SRS (bottom) images; and fused images.

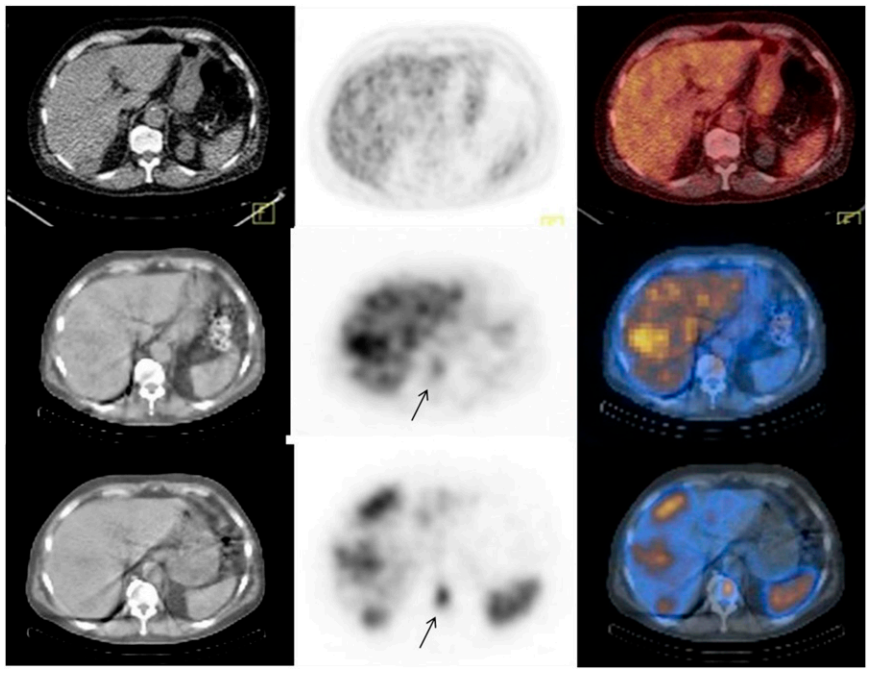

FIGURE 3. Patient in whom SRS and ^{123}I-MIBG scintigraphy were superior to ^{18}F-FDG PET. Patient had ileal neuroendocrine tumor, and Ki67 index was below 2%. Both SRS and ^{123}I-MIBG scintigraphy revealed at least 3 liver metastases and a bone metastasis (arrow). SRS also identified several lymph node metastases in retroperitoneum. ^{18}F-FDG PET findings were negative. From left to right are CT images; ^{18}F-FDG PET (top), ^{123}I-MIBG scintigraphy (middle), and SRS (bottom) images; and fused images.

Besides the high sensitivity of ^{18}F-FDG PET for highly proliferating tumors, there was no significant difference in the ability of SRS and ^{18}F-FDG PET to detect lymph node metastases, which often are small lesions. This finding could be explained by the superior sensitivity and spatial resolution achievable with PET, compared with SPECT, enabling the detection of smaller lesions. Therefore, newly developed tracers based on radiolabeled somatostatin analogs for PET, such as ^{68}Ga-DOTATOC, could potentially replace the currently used ^{111}In-octreotide (*10,15*). As illustrated by the patient in Figure 4, ^{18}F-FDG PET could perhaps be used as an alternative to ^{111}In-octreotide when PET-based somatostatin tracers are lacking. Finding these cases is relevant because surgical intervention may be a treatment option for patients with less disseminated disease. In the present study, as shown in Table 3, 6 of the 11 SRS-negative tumors were at or below 2 cm. Of these, only 2 were ^{18}F-FDG PET–positive whereas 4 of the ^{18}F-FDG PET–positive tumors were larger than 3 cm. The overall sensitivities were relatively high in our study (89%, 52%, and 58% for SRS, ^{123}I-MIBG scintigraphy, and ^{18}F-FDG PET, respectively), compared with other studies (*4*), probably because of the addition of SPECT image acquisition and low-dose CT, which has been shown to increase the accuracy of detection and localization of pathologic foci (*30,31*). However, with the recent introduction of high-resolution CT cameras in combination with PET and γ-cameras, the overall diagnostic sensitivity and accuracy are likely to increase further.

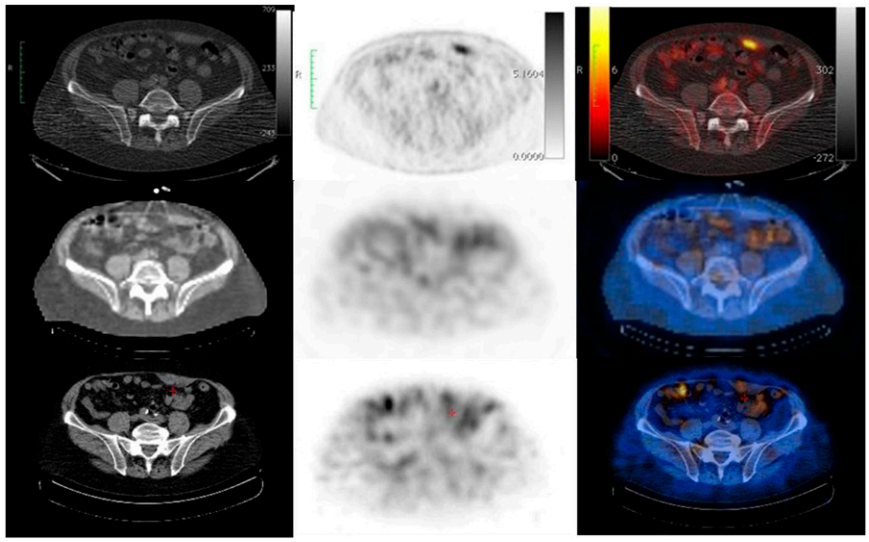

FIGURE 4. Patient in whom ^{18}F-FDG PET was superior to SRS and ^{123}I-MIBG scintigraphy. Patient had neuroendocrine colon carcinoma, and Ki67 index was 95%. ^{18}F-FDG PET revealed focus in abdominal wall. Both SRS and ^{123}I-MIBG scintigraphy had negative findings. From left to right are CT images; ^{18}F-FDG PET (top), ^{123}I-MIBG scintigraphy (middle), and SRS (bottom) images; and fused images.

Recent consensus reports highlight the importance of type-specific treatment because of the biologic diversity of these tumors (*16,32*). Based on the region of origin of the neuroendocrine tumors, the sensitivity of ^{123}I-MIBG scintigraphy (71%) for detection of ileal neuroendocrine tumors was superior to that of ^{18}F-FDG PET (36%), whereas the opposite was true for the pancreaticoduodenal neuroendocrine tumors, with sensitivities of 31% and 79% for ^{123}I-MIBG scintigraphy and ^{18}F-FDG PET, respectively. For both the ileal neuroendocrine tumors and the pancreaticoduodenal neuroendocrine tumors, the sensitivity of SRS exceeded that of ^{123}I-MIBG scintigraphy and ^{18}F-FDG PET. This finding agrees with previous findings by others (*6*). Compared with other tracers targeting molecules of the monoamine pathways, the sensitivity of ^{123}I-MIBG scintigraphy was low for all tumor subtypes. Tracers such as 6-^{18}F-fluoro-L-dihydroxyphenylalanine and ^{11}C-5-hydroxytryptophan may be more widely applicable and could become important supplements to somatostatin-labeled analogs (*13*). However, these tracers are still not as universally available and have, to the best of our knowledge, not been labeled with β-emitting isotopes for radionuclide therapy. Today, neuroendocrine tumors can be treated with targeted radionuclide therapy based on either somatostatin analogs labeled with ^{177}Lu or ^{90}Y or MIBG labeled with ^{131}I (*33,34*). Therefore, precise knowledge of the tumor biology of different neuroendocrine tumor subgroups is crucial for selection of the optimal treatment strategy for each patient. Although ^{123}I-MIBG scintigraphy has an overall lower sensitivity than SRS for detection of neuroendocrine tumors, and treatment based on somatostatin labeled with ^{177}Lu or ^{90}Y is much more commonly used, ^{131}I-MIBG radionuclide treatment might be relevant for selected patients if the tracer accumulation of ^{123}I-MIBG exceeds the octreotide accumulation.

In the present study we found only three ^{123}I-MIBG scintigraphy–positive patients who were SRS-negative, and we found ^{123}I-MIBG scintigraphy to have no added value in SRS-positive patients. Therefore, we doubt that ^{123}I-MIBG scintigraphy will have a role in neuroendocrine tumor imaging and treatment unless the patient is known to have disseminated disease and negative SRS findings. ^{18}F-FDG PET, on the other hand, may become important for high-grade neuroendocrine tumors. Additionally, the strong association with the aggressiveness of the tumor suggests that ^{18}F-FDG PET could be valuable for selecting treatment, monitoring therapy, and determining prognosis. This role of ^{18}F-FDG PET is well documented for other types of cancer, such as Hodgkin disease and colorectal cancer (*35,36*).

CONCLUSION

The overall sensitivity for ^{123}I-MIBG scintigraphy and ^{18}F-FDG PET was low compared with SRS. However, the sensitivity of ^{18}F-FDG PET was high for pancreaticoduodenal and poorly differentiated neuroendocrine carcinomas. The results indicate that although SRS should still be considered the routine method, ^{18}F-FDG PET provides complementary diagnostic information and could become the diagnostic scintigraphy technique of choice for pancreaticoduodenal and poorly differentiated neuroendocrine carcinomas if SRS findings are negative. However, because ^{18}F-FDG PET provides complementary information—for example, prognostic information—it may well become useful also for SRS-positive tumors. The sensitivity of ^{123}I-MIBG scintigraphy was low, and its future role in neuroendocrine tumors seems limited.

ACKNOWLEDGMENTS

Financial support from the Danish Cancer Society, the Danish Medical Research Council, the AP Moller Foundation, and the John and Birthe Meyer Foundation is gratefully acknowledged. The staffs of the Department of Clinical Physiology, Nuclear Medicine and PET and the Department of Surgical Gastroenterology are gratefully acknowledged for their work on the project.

REFERENCES

1. Binderup T, Knigge U, Mogensen AM, Hansen CP, Kjaer A. Quantitative gene expression of somatostatin receptors and noradrenaline transporter underlying scintigraphic results in patients with neuroendocrine tumors. *Neuroendocrinology.* 2008;87:223–232.
2. Reubi JC, Waser B, Schaer JC, Laissue JA. Somatostatin receptor sst1-sst5 expression in normal and neoplastic human tissues using receptor autoradiography with subtype-selective ligands. *Eur J Nucl Med.* 2001;28:836–846.
3. Srirajaskanthan R, Watkins J, Marelli L, Khan K, Caplin ME. Expression of somatostatin and dopamine 2 receptors in neuroendocrine tumours and the potential role for new biotherapies. *Neuroendocrinology.* 2009;89:308–314.
4. Koopmans KP, Neels ON, Kema IP, et al. Molecular imaging in neuroendocrine tumors: molecular uptake mechanisms and clinical results. *Crit Rev Oncol Hematol.* 2009;71:199–213.
5. Raderer M, Kurtaran A, Leimer M, et al. Value of peptide receptor scintigraphy using ^{123}I-vasoactive intestinal peptide and ^{111}In-DTPA-D-Phe1-octreotide in 194 carcinoid patients: Vienna University Experience, 1993 to 1998. *J Clin Oncol.* 2000;18:1331–1336.
6. Ezziddin S, Logvinski T, Yong-Hing C, et al. Factors predicting tracer uptake in somatostatin receptor and MIBG scintigraphy of metastatic gastroenteropancreatic neuroendocrine tumors. *J Nucl Med.* 2006;47:223–233.
7. Von Moll L, McEwan AJ, Shapiro B, et al. Iodine-131 MIBG scintigraphy of neuroendocrine tumors other than pheochromocytoma and neuroblastoma. *J Nucl Med.* 1987;28:979–988.
8. Adams S, Baum RP, Hertel A, Schumm-Drager PM, Usadel KH, Hor G. Metabolic (PET) and receptor (SPET) imaging of well- and less well-differentiated tumours: comparison with the expression of the Ki-67 antigen. *Nucl Med Commun.* 1998;19:641–647.
9. Belhocine T, Foidart J, Rigo P, et al. Fluorodeoxyglucose positron emission tomography and somatostatin receptor scintigraphy for diagnosing and staging carcinoid tumours: correlations with the pathological indexes p53 and Ki-67. *Nucl Med Commun.* 2002;23:727–734.
10. Kayani I, Bomanji JB, Groves A, et al. Functional imaging of neuroendocrine tumors with combined PET/CT using ^{68}Ga-DOTATATE (DOTA-DPhe1,Tyr3-octreotate) and ^{18}F-FDG. *Cancer.* 2008;112:2447–2455.
11. Buck AK, Schirrmeister H, Hetzel M, et al. 3-deoxy-3-[^{18}F]fluorothymidine-positron emission tomography for noninvasive assessment of proliferation in pulmonary nodules. *Cancer Res.* 2002;62:3331–3334.
12. Takei T, Kuge Y, Zhao S, et al. Enhanced apoptotic reaction correlates with suppressed tumor glucose utilization after cytotoxic chemotherapy: use of ^{99m}Tc-annexin V, ^{18}F-FDG, and histologic evaluation. *J Nucl Med.* 2005;46:794–799.
13. Koopmans KP, Neels OC, Kema IP, et al. Improved staging of patients with carcinoid and islet cell tumors with ^{18}F-dihydroxy-phenyl-alanine and

^{11}C-5-hydroxy-tryptophan positron emission tomography. *J Clin Oncol.* 2008; 26:1489–1495.
14. Koopmans KP, de Vries EG, Kema IP, et al. Staging of carcinoid tumours with ^{18}F-DOPA PET: a prospective, diagnostic accuracy study. *Lancet Oncol.* 2006;7: 728–734.
15. Buchmann I, Henze M, Engelbrecht S, et al. Comparison of ^{68}Ga-DOTATOC PET and ^{111}In-DTPAOC (OctreoScan) SPECT in patients with neuroendocrine tumours. *Eur J Nucl Med Mol Imaging.* 2007;34:1617–1626.
16. Plockinger U, Rindi G, Arnold R, et al. Guidelines for the diagnosis and treatment of neuroendocrine gastrointestinal tumours: a consensus statement on behalf of the European Neuroendocrine Tumour Society (ENETS). *Neuroendocrinology.* 2004;80:394–424.
17. Rappeport ED, Hansen CP, Kjaer A, Knigge U. Multidetector computed tomography and neuroendocrine pancreaticoduodenal tumors. *Acta Radiol.* 2006;47:248–256.
18. Dobbeleir AA, Hambye AS, Franken PR. Influence of high-energy photons on the spectrum of iodine-123 with low- and medium-energy collimators: consequences for imaging with ^{123}I-labelled compounds in clinical practice. *Eur J Nucl Med.* 1999;26:655–658.
19. Bombardieri E, Aktolun C, Baum RP, et al. ^{131}I/^{123}I-metaiodobenzylguanidine (MIBG) scintigraphy: procedure guidelines for tumour imaging. *Eur J Nucl Med Mol Imaging.* 2003;30:BP132–BP139.
20. Kloppel G, Perren A, Heitz PU. The gastroenteropancreatic neuroendocrine cell system and its tumors: the WHO classification. *Ann N Y Acad Sci.* 2004;1014:13–27.
21. Fiebrich HB, Brouwers AH, Kerstens MN, et al. 6-[F-18]Fluoro-L-dihydroxyphenylalanine positron emission tomography is superior to conventional imaging with ^{123}I-metaiodobenzylguanidine scintigraphy, computer tomography, and magnetic resonance imaging in localizing tumors causing catecholamine excess. *J Clin Endocrinol Metab.* 2009;94:3922–3930.
22. Therasse P, Arbuck SG, Eisenhauer EA, et al. New guidelines to evaluate the response to treatment in solid tumors. European Organization for Research and Treatment of Cancer, National Cancer Institute of the United States, National Cancer Institute of Canada. *J Natl Cancer Inst.* 2000;92:205–216.
23. Modlin IM, Lye KD, Kidd M. A 5-decade analysis of 13,715 carcinoid tumors. *Cancer.* 2003;97:934–959.
24. Yao JC, Hassan M, Phan A, et al. One hundred years after "carcinoid": epidemiology of and prognostic factors for neuroendocrine tumors in 35,825 cases in the United States. *J Clin Oncol.* 2008;26:3063–3072.
25. Oberg K, Astrup L, Eriksson B, et al. Guidelines for the management of gastroenteropancreatic neuroendocrine tumours (including bronchopulmonary and thymic neoplasms). Part I—general overview. *Acta Oncol.* 2004;43: 617–625.
26. Kaltsas G, Korbonits M, Heintz E, et al. Comparison of somatostatin analog and meta-iodobenzylguanidine radionuclides in the diagnosis and localization of advanced neuroendocrine tumors. *J Clin Endocrinol Metab.* 2001;86:895–902.
27. Kwekkeboom DJ, Mueller-Brand J, Paganelli G, et al. Overview of results of peptide receptor radionuclide therapy with 3 radiolabeled somatostatin analogs. *J Nucl Med.* 2005;46(suppl 1):62S–66S.
28. Rindi G, Kloppel G, Couvelard A, et al. TNM staging of midgut and hindgut (neuro) endocrine tumors: a consensus proposal including a grading system. *Virchows Arch.* 2007;451:757–762.
29. Rindi G, Kloppel G, Alhman H, et al. TNM staging of foregut (neuro)endocrine tumors: a consensus proposal including a grading system. *Virchows Arch.* 2006; 449:395–401.
30. Perri M, Erba P, Volterrani D, et al. Octreo-SPECT/CT imaging for accurate detection and localization of suspected neuroendocrine tumors. *Q J Nucl Med Mol Imaging.* 2008;52:323–333.
31. Krausz Y, Keidar Z, Kogan I, et al. SPECT/CT hybrid imaging with ^{111}In-pentetreotide in assessment of neuroendocrine tumours. *Clin Endocrinol (Oxf).* 2003;59:565–573.
32. Oberg K, Astrup L, Eriksson B, et al. Guidelines for the management of gastroenteropancreatic neuroendocrine tumours (including bronchopulmonary and thymic neoplasms). Part II—specific NE tumour types. *Acta Oncol.* 2004;43: 626–636.
33. van Essen M, Krenning EP, Kam BL, de JM, Valkema R, Kwekkeboom DJ. Peptide-receptor radionuclide therapy for endocrine tumors. *Nat Rev Endocrinol.* 2009;5:382–393.
34. Zuetenhorst H, Taal BG, Boot H, Valdes OR, Hoefnagel C. Long-term palliation in metastatic carcinoid tumours with various applications of meta-iodobenzylguanidine (MIBG): pharmacological MIBG, ^{131}I-labelled MIBG and the combination. *Eur J Gastroenterol Hepatol.* 1999;11:1157–1164.
35. de Geus-Oei LF, Ruers TJ, Punt CJ, Leer JW, Corstens FH, Oyen WJ. FDG-PET in colorectal cancer. *Cancer Imaging.* 2006;6(suppl):S71–S81.
36. Hutchings M, Loft A, Hansen M, et al. FDG-PET after two cycles of chemotherapy predicts treatment failure and progression-free survival in Hodgkin lymphoma. *Blood.* 2006;107:52–59.

The Journal of NUCLEAR MEDICINE

Functional Imaging of Neuroendocrine Tumors: A Head-to-Head Comparison of Somatostatin Receptor Scintigraphy, ^{123}I-MIBG Scintigraphy, and ^{18}F-FDG PET

Tina Binderup, Ulrich Knigge, Annika Loft, Jann Mortensen, Andreas Pfeifer, Birgitte Federspiel, Carsten Palnaes Hansen, Liselotte Højgaard and Andreas Kjaer

J Nucl Med. 2010;51:704-712.
Published online: April 15, 2010.
Doi: 10.2967/jnumed.109.069765

The Journal of Nuclear Medicine is published monthly.
SNMMI | Society of Nuclear Medicine and Molecular Imaging
1850 Samuel Morse Drive, Reston, VA 20190.
(Print ISSN: 0161-5505, Online ISSN: 2159-662X)

SNMMI SOCIETY OF NUCLEAR MEDICINE AND MOLECULAR IMAGING